VILNIUS TECH
Vilnius Gediminas Technical University

▌AVIATION

DEVELOPING ALSIM AL250 BASED eVTOL FLIGHT SIMULATOR

Vilius PORTAPAS ⓘ ✉

Faculty of Engineering, University of Nottingham, Nottingham, United Kingdom

Abstract. A novel eVTOL aircraft simulator was developed for research and teaching purposes. The simulator integrated MATLAB/Simulink flight dynamics model with Alsim AL250 FNPT II flight simulator. Simplified version of the Neoptera's eOpter eVTOL aircraft was used as a test case to verify the flight simulator. It was shown that the aircraft responded as expected by the pilot and that the traditional handling qualities metrics and VTOL requirements (MIL-F-83300, MIL-F-8785C, EASA-SC-VTOL-02) could be used along the flight simulator to assess aircraft being tested. Take-off showed an increase in climb rate as well as overshoot of the target altitude with higher RPM setting. Qualitative assessment of transition showed suitable stability and control feel for the eVTOL to be operated by a single pilot. Quantitative assessment of the longitudinal manoeuvring characteristics showed Level 2 SPPO handling qualities for the tested eVTOL aircraft, qualitative definition of which agreed with the pilot's opinion. It was also shown that increasing initial velocity for the SPPO mode test increased the mode's natural frequency, but almost did not affect the damping ratio, which is within the expectations.

1. Introduction

The eVTOL industry has proliferated in the recent decade, evidenced by the increasing number of eVTOL designs. The World eVTOL Aircraft Directory, started by the Vertical Flight Society in 2016, currently counts 1100+ eVTOL designs (Vertical Flight Society, 2024). Around 50% of them are based on thrust-borne take-off and landing, and wing-borne cruise flight. As such all of them introduce an intermediary flight regime – transition – that happens when an aircraft transits between the vertical and horizontal flight and requires a configuration change by tilting some parts, e.g. rotors, motors, wing(s), to vector the thrust.

Generally, VTOL flight is well known to the military community, which has accumulated more than three decades of VTOL flying experience. British Aerospace Harrier GR9, Bell Boeing V-22 Osprey and Lockheed Martin F-35B Lightning are the best-known types of VTOL military aircraft. However, their purpose and size are significantly different from the civil ones, which is clearly evidenced by the operational environment and MTOM. While the operating environment ranges from the aircraft carriers to the most unpredictable landing sites for the military VTOLs, it is widely accepted that the civil eVTOLs will be flying within the urban environment from/to the well-defined vertiports (Midlands Aerospace Alliance, Lichfields, Achiev-

ing the Difference, 2024). The maximum take-off mass and payload are another significant differences: MTOM of military VTOLs is circa 20 tons versus ca. 3 tons for eVTOLs, while the payload varies between ca. 7 tons for military VTOLs versus ca. 450 kg for eVTOLs. Finally, the biggest differences between military VTOLs and civil eVTOLs are their propulsion systems and modes of flying – while military VTOLs use kerosene type jet fuels and are piloted, the eVTOLs will use electricity and will be autonomous.

All the differences mentioned above, i.e. size, operational environment, propulsion system, create a significant knowledge gap between the principles of flying large VTOLs and small eVTOLs. Hence, the civil aviation community is building its knowledge and experience based on the use of helicopters for vertical flight and small aeroplanes for horizontal flight. Helicopters use thrust vectoring to fly, but this experience is practically unapplicable to eVTOLs due to no change between thrust-borne and wing-borne flight modes. The transition phase is deemed as the most challenging flight regime for the civil eVTOLs. Although the industry anticipates that the future eVTOLs will be autonomous and, hence, control systems will control the entire flight profile, it also agrees that the first flights will be piloted to further understand the flying and handling qualities of such aircraft. Hence, both industry and society need simulation tools

that allow 1) pilot-in-the-loop simulations of eVTOLs, 2) developing of control systems for eVTOLs, and 3) advancing research into and understanding of eVTOL flight.

Numerous flight dynamic models have been developed to model and simulate different eVTOL configurations (Abà et al., 2020; Simmons, 2023; Zhao et al., 2024). However, there is only a handful of pilot-in-the-loop capable reconfigurable-into-eVTOL and eVTOL flight simulators (Díaz García et al., 2021; Padfield & White, 2003), although flight simulators have been used to analyse flight aspects of large military VTOLs for more than four decades (Churchill & Dugan, 1982; Decker, 2001). Largest eVTOL developers have their own simulation tools, which are not available for public access and research. As a result, the most of research papers on eVTOL flight simulations refer to simple PC-based simulators that do not provide full cockpit environment. Hence, it is currently almost impossible to investigate 1100+ eVTOL designs for their flying and handling qualities through the piloted simulation trials. Moreover, a modelling and simulation framework capable of pilot-in-the-loop testing, similar to CA^{2}LM (Portapas et al., 2016; Portapas & Cooke, 2020), that allows rapid aircraft model configuration changes is needed to investigate different currently existing eVTOLs and to support the development of the future eVTOL designs.

This paper presents the development of such rapidly reconfigurable eVTOL flight simulation framework. It uses the MATLAB/Simulink package to model the flight dynamics of an eVTOL integrated with the Alsim AL250 flight simulator to provide the cockpit environment for the piloted simulation trials. It also presents a case study of eVTOL trials as a verification exercise for the simulation framework. It is important to note that the scope of this eVTOL flight simulation framework is to provide a modular research and teaching tool that enables implementation of variable fidelity (e)VTOL models, allows development of flight control systems and other eVTOL research activities. It is not the scope of this simulation framework to reproduce high-fidelity model of any currently flying eVTOL as the test data for such aircraft is not publicly available.

2. Methodology

The proposed eVTOL flight simulation framework integrates MATLAB/Simulink based flight dynamics model with the cockpit environment within the Alsim AL250 flight simulator. This section provides a quick overview of the eVTOL flight dynamics model, presents the peculiarities of its integration with the Alsim AL250 flight simulator and suggests the verification procedure. It is important to emphasise that the validation of such a simulator is currently impossible as there are no publicly available flight test data for eVTOL aircraft.

The Neoptera's eOpter eVTOL aircraft (Didey, 2020) was used as an example. It is a tandem-wing aircraft consisting of a detachable lifecell (cabin) and an airframe consisting of two wings attached to the frame. Each wing is equipped

with four electric motors that drive eight propellers in total. The airframe rotates around the cabin when transitioning from vertical to horizontal flight and vice versa. Potential concept of operations of this eVTOL was defined by Portapas et al. (2021), and the technical specifications of this eVTOL were provided by Portapas and Zaidi (2022).

Extensive analysis of this airframe showed that it is inherently unstable and, hence, requires a complex control system, which would prevent analysing flying and handling qualities of the bare airframe. It was decided to simplify the numerical model by fixing the airframe to the cabin, and instead rotating only the motors rather than the whole airframe.

2.1. Flight dynamics model

One of the objectives of the research project presented in this paper was to understand the requirements of the human-machine interface for the eVTOL flight simulator. Hence, the flight dynamics model, including aerodynamics and other components, is not required to be of high fidelity or represent any realistic eVTOL aircraft. It rather must provide bare minimum to allow a pilot to take off vertically, transition to a horizontal flight, perform cruise flight, transition back to vertical flight and land vertically. As such, a very simplistic aerodynamic model was developed and only three longitudinal degrees of freedom, i.e. surge, heave and pitch, were modelled to simplify the initial analysis of the piloted eVTOL flight.

MATLAB/Simulink environment was chosen for the flight dynamics model to be developed as:

- it allows quick changes to be made for a vehicle under investigation;
- it allows the implementation of multiple vehicles and their parameters in an easy-to-use plug-and-play environment;
- it is easy to learn for every engineer without requiring special knowledge of programming, hence it is broadly used across the aerospace engineering domain;
- it enables further developments of the model within academia and industry.

Aerodynamic forces and moments are calculated for the forward and rear wings, and the cabin. Both wings contribute to the lift (during the horizontal flight) and drag forces, while the cabin contributes only to the drag force. Aerofoil lift, drag and pitching moment coefficients ($C_L(Re, \alpha)$, $C_D(Re, \alpha)$ and $C_{m0}(Re, \alpha)$) were generated using JavaFoil v2.28 software, which uses the potential flow method and Prandtl's lifting line theory approximation for the finite wing (Hepperle, 2017). Each aerodynamic coefficient is a function of the Reynolds number Re and the angle of attack α of the wing and is retrieved from the 2-D lookup tables. Aerodynamics of elevons are modelled by constant lift and drag components ($C_L(\delta_{elev})$ and $C_D(\delta_{elev})$) added to the corresponding coefficients of each wing. Aerodynamic coefficients of elevons are scaled with respect to the area of each wing rather than the area of each elevon. The lift L,

drag D and aerodynamic pitching moment M_0 of each wing and the drag of the cabin D_c are then expressed as:

$$\begin{bmatrix} L \\ D \\ M_0 \end{bmatrix}_w = \begin{bmatrix} C_L\left(\mathrm{Re},\alpha\right)+C_{L_{\delta_{elev}}}\delta_{elev} \\ C_D\left(\mathrm{Re},\alpha\right)+C_{D_{\delta_{elev}}}\delta_{elev} \\ \overline{c}C_{m0}\left(\mathrm{Re},\alpha\right) \end{bmatrix}\overline{q}\int_{-\frac{b}{2}}^{\frac{b}{2}}c\left(y\right)dy; \quad (1a)$$

$$D_c = \overline{q}C_D\left(cabin\right)S_{ref}, \quad (1b)$$

where b is the span of a wing, $c(y)$ – chord length at spanwise position, $\overline{c}$ – mean aerodynamic chord of a wing, $\overline{q} = \dfrac{\rho V^2}{2}$ – dynamic pressure (where ρ – air density, V – airspeed), δ_{elev} – elevon deflection angle, $C_D(cabin)$ – drag coefficient of the cabin, which is assumed to be constant, and S_{ref} – reference area of the cabin.

The aerodynamic forces calculated in the wind axes system must be converted into the body axis system for further processing. This is a one-step conversion (angle of attack α) for the lift and drag generated by the wing (assuming zero wing incidence angle) and for cabin drag as shown below:

$$\vec{F}_{b,w,c} = \begin{bmatrix} F_x \\ F_y \\ F_z \end{bmatrix}_b = \begin{bmatrix} -\cos\alpha & 0 & \sin\alpha \\ 0 & 0 & 0 \\ \sin\alpha & 0 & -\cos\alpha \end{bmatrix}\begin{bmatrix} D \\ 0 \\ L \end{bmatrix}_{w,c}, \quad (2)$$

where $\vec{F}_b = \begin{bmatrix} F_x & F_y & F_z \end{bmatrix}_b^T$ is the force vector in the body axis system.

The total pitching moment due to aerodynamic forces consists of the aerodynamic pitching moment around quarter chord point M_0 and contributions from the forces acting on each wing i due to their displacement from the aircraft CG:

$$M_{y,w} = \sum_{i=1}^{2}M_{y,i} = M_{0,i}+F_{x,i}\left(z_{ac,i}-z_{cg}\right)-F_{z,i}\left(x_{ac,i}-x_{cg}\right); (3a)$$

$$M_{y,c} = F_{x,c}\left(z_{ac,c}-z_{cg}\right)-F_{z,c}\left(x_{ac,c}-x_{cg}\right). \quad (3b)$$

Propulsion forces and moments are calculated for all eight propellers. Each propeller is driven by an electric motor. However, currently there are no propulsion system dynamics to model the input latency, meaning that the input made by a pilot in the cockpit is directly and instantly translated into change of the thrust. All propellers have three blades of Clark Y section at 20° blade angle and are referred to as 5868-9 by (Hartman & Biermann, 1938). Total thrust T_p produced by all eight propellers is a sum of the thrust of each propeller j as follows:

$$T_{p,j} = C_{T,j}\left(J_j\right)\rho n_j^2 d_j^4, \quad (4)$$

where $C_T(J)$ is propeller thrust coefficient as a function of the propeller advance ratio $J = \dfrac{V}{nd}$, where n is revolutions per second of a propeller, d – propeller diameter.

The resulting force components in the body axis system depend on each propeller incidence angle θ_j and are calculated as follows:

$$\vec{F}_{b,p,j} = \begin{bmatrix} F_x \\ F_y \\ F_z \end{bmatrix}_{b,j} = \begin{bmatrix} \cos\theta_j & 0 & \sin\theta_j \\ 0 & 0 & 0 \\ -\sin\theta_j & 0 & \cos\theta_j \end{bmatrix}\begin{bmatrix} T_{p,j} \\ 0 \\ 0 \end{bmatrix}. \quad (5)$$

The total pitching moment due to engine is calculated as a sum of pitching moment contributions of each engine j:

$$M_{y,p} = \sum_{j=1}^{8}M_{y,j} = F_{x,j}\left(z_j-z_{cg}\right)-F_{z,j}\left(x_j-x_{cg}\right). \quad (6)$$

Total forces and moments acting on the eVTOL aircraft are calculated as follows:

$$\vec{F}_b = \vec{F}_{b,w}+\vec{F}_{b,c}+\vec{F}_{b,p}+\vec{F}_{b,g}; \quad (7a)$$

$$M_y = M_{y,w}+M_{y,c}+M_{y,p}+M_{y,g}. \quad (7b)$$

Moment due to gravity $M_{y,g}$ is zero due to the gravity force acting through the CG. CG of the aircraft under analysis has been adjusted so that the pitching moment generated by the propulsion forces $M_{y,p}$ is zero as well. Hence, the only non-zero pitching moment components are due to the aerodynamic forces of the cabin and the wings. It is important to note here that the moment generated by the wings is orders of magnitude greater than that generated by the cabin.

Conversion from the thrust-borne to the wing-borne configuration is done by pivoting only the engines rather than the whole airframe as shown in Figure 1. Although it is a significant simplification when compared to the original eVTOL configuration, it allows to maintain the stability of the aircraft without any flight control system, hence reducing the complexity of the model being used in teaching about and further research into the eVTOL flight peculiarities.
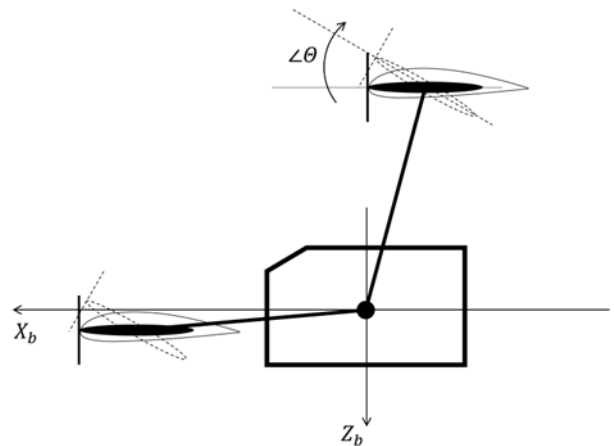

Figure 1. Schematics of the engine rotation of the eVTOL model under investigation

42

V. Portapas. Developing Alsim AL250 based eVTOL flight simulator

2.2. Alsim AL250 flight simulator

Alsim AL250 is classified as the flight and navigation procedures trainer II (FNPT II) flight simulator as defined by (European Aviation Safety Agency [EASA], 2012) and is usually used in the pilot training process. It provides a cockpit environment that represents a generic multi-engine general aviation aeroplane. Hardware part consists of a cockpit with all the relevant systems, e.g. avionics, control inceptors, and visualisation tools, while the software part provides multiple functions to run the systems to simulate different aircraft. Functions exchange variables between each other through the so-called data pool, i.e. each function imports the needed variables from and exports the calculated variables to the data pool. A set of validated functions, including the ones calculating states of an aeroplane related to the flight dynamics, forms a generic aircraft model.

Alsim's Engineering Pack is a PC with a direct connection to the flight simulator's system and its data pool. It allows importing the control inputs (and other variables if needed) from the data pool into the MATLAB/Simulink model and exporting the calculated states of an aircraft from the model into the data pool for further processing and visualisation. Hence, the preprogrammed validated aircraft (flight dynamics) model is bypassed by the MATLAB/Simulink model, while the hardware and other software parts are used as usual to generate the environment. This approach allows modelling and simulation of any aircraft with the only limitation being the non-reconfigurable cockpit environment.

Control inceptors and their arrangement differ among aircraft types. Alsim AL250 is equipped with standard control inceptors for a twin-engine aeroplane, i.e. yoke for pitch and roll control, pedals for yaw control and throttle quadrant for engine control. The eVTOL simulation framework must be built around these control inceptors as they are fixed. Hence, yoke and pedals would be used as usual to control roll, pitch and yaw.

Pitch and engine controls are the only control variables for the current 3-DoF eVTOL implementation. Pitch control is implemented in a way that pushing the yoke creates negative (nose down) moment, i.e. deflects the forward elevons up and rear elevons down as CG is between the forward and rear wings. Engine controls are based on two left (black) levers for throttle, two middle (blue) levers for blade pitch angle and two right (red) levers for air-fuel mixture ratio as shown in Figure 2.

Currently, only the left throttle (black) lever is used to control the thrust by directly adjusting the rotational speed of all eight motors in the current eVTOL implementation. This means that the lever directly controls the rotational speed of each propeller as there is no gearing (dynamics) between the motor and the propeller modelled. Assuming the range of the throttle lever from zero (0%) to one (100%), the propeller RPM function is:

$$RPM_{prop} = RPM_{motor} = n * \delta_t, \qquad (8)$$

where n is the nominal rotational speed in revolutions per minute and δ_t is throttle input (0–1).
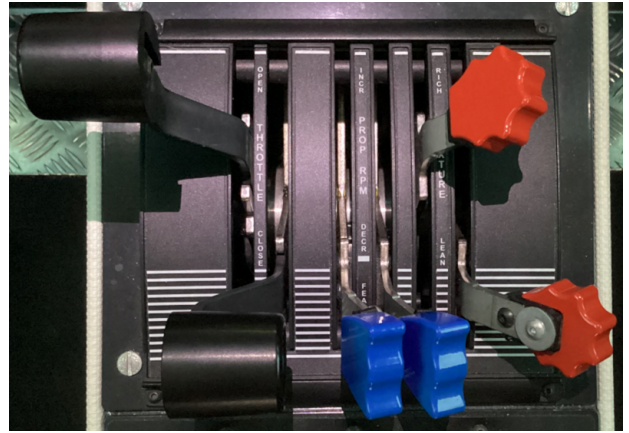

Figure 2. Throttle quadrant of Alsim AL250

The left mixture ratio (red) lever is used to change the propeller incidence angle, i.e. it rotates the thrust vector in the model. It was decided to implement the eVTOL configuration change this way as the two mixture ratio levers used in the internal combustion engines become meaningless in case of electric motors. The full aft position of the lever means the engines are perpendicular to the wings and, hence, create a vertical force pointing upwards along the Z_b axis. The full forward position of the lever means the engines are parallel to wings and, hence, create a horizontal force pointing forwards along the X_b axis (see Figure 1).

The blade pitch angle levers were left unused as the modelled eVTOL aircraft is equipped with fixed-pitch blade propellers. However, there are electric aircraft in development that have variable-pitch propellers and, hence, it was decided that it is the best practice to leave the levers for controlling the blade pitch angle in future designs.

Understandably, such a cockpit environment of a twin-engine general aviation aeroplane does not represent the future eVTOL cockpit environment. However, such approach supports identification of information and instruments required by a pilot to fly such aircraft. Moreover, it provides traditional control inceptors, i.e. yoke, pedals, engine levers, to understand the needs of pilots transitioning from fixed wing to eVTOL aircraft.

2.3. Verification of the eVTOL flight simulation framework

Verification of the eVTOL flight simulator is a vital step to ensure that the control inceptors provide the correct signals to which an aircraft responds as expected by a pilot when making a control input. This means that 1) the pilot inputs must be read correctly, and 2) the flight dynamics must be modelled correctly. The only known pilot expectations can be associated with fixed and rotary wing aircraft, i.e. horizontal and vertical flight phases of an eVTOL aircraft. The transition flight phase of the small eVTOLs is not yet known for the civil aviation community, hence there are no references of what to expect. However, a common pilot sense based on their experience allows

to set expectations for the aircraft behaviour within this phase. Moreover, eVTOLs are powered by multiple electric motors, which make them to respond immediately to a throttle input, hence removing the usual delay of internal combustion engines and introducing further complexity into the overall behaviour of eVTOLs.

The simplification of an eVTOL aircraft model was, hence, paramount to reduce the complexity and to isolate as much unpredictability as possible. Isolating and testing the unknowns one by one was the only possible way to verify the simulation framework. Hence, an expectable level of flight regimes was the reason for having a simplified eVTOL aircraft model programmed into the simulation framework.

Following the above reasoning, the verification of the eVTOL flight simulator was approached by using the author's piloting experience and differentiating the process into the following sections:

- checking control inceptors – the procedure that pilots do before every flight to ensure that controls are responding as expected, e.g. pushing the yoke forward deflects elevons in a way that creates pitching down moment;
- simulating vertical take-off with different engine (RPM) setting to check that climb rate changes as expected, e.g. climb rate is higher for higher RPM setting and vice versa;
- simulating transition from vertical to horizontal flight with different initial engine (RPM) setting to check that the aircraft performance changes as expected, e.g. rotating the engines from the vertical to the horizontal position increases the horizontal velocity component and reduces the vertical velocity;
- simulating the short period pitching oscillation (SPPO) mode to check that the dynamic response of the eVTOL is within the expectations based on the traditional fixed wing aircraft.

Firstly, with the eVTOL stationary on the ground, the elevon, throttle and frame angle levers were checked. It was expected that the inputs into the flight dynamics model would follow the input signal from the control inceptors with no delay or offset as there were no control dynamics modelled.

Secondly, the vertical take-off and transition exercise was performed. The transition was initiated by simultaneously increasing RPM and starting to continuously reduce angle of motors from 90° to 0° once the aircraft reached 500 ft (ca. 150 m) AAL. The target altitude was 1000 ft (ca. 300 m) AAL. It was anticipated that the higher take-off RPM setting would result in higher vertical speed (climb rate) and the subsequent overshoot of the target altitude. It was also expected that the horizontal velocity would increase during the transition due to the thrust vector being rotated from the vertical to the horizontal position. Chalk et al. (1971) argues that it is possible to determine only qualitative requirements based on a mission profile for the transition phase. Hence, both take-off and transition phases were assessed rather qualitatively as the real world data for this eVTOL aircraft was not available.

Finally, the SPPO mode, which is the longitudinal dynamic mode of rapidly changing AoA, was tested in terms of the mode's damping ratio and natural frequency for the given eVTOL aircraft configuration to investigate the fidelity of the flight dynamics model. Model's ability to follow the expected AoA changes means that the flight dynamics model and the simulator itself is of acceptable fidelity. It was expected for the mode to be stable, i.e. damped, as the aircraft CG position was set in front of the neutral point of the aircraft, compensating for the lift curve slope of the forward wing being slightly greater than of the rear wing (Portapas & Zaidi, 2022). The rear wing acts as a horizontal stabiliser in such arrangement as is the case for the traditional aeroplane configurations. Hence, the eVTOL aircraft under investigation was considered an aeroplane for the horizontal flight, and the parameters of the SPPO mode were compared against the requirements within the military specifications MIL-F-8785C (Moorhouse & Woodcock, 1981), which is the usual practice within the aerospace engineering research community. Moreover, the data from the non-linear simulations were compared against the linearised SPPO approximations from Nelson (1998) and Schoser et al. (2022). Nelson (1998) approximates SPPO natural frequency and damping ratio as the functions depending on derivatives: $\omega_n = f\left(M_\alpha, M_q, Z_\alpha, u_0\right)$ and $\zeta = f\left(M_{\dot{\alpha}}, M_q, Z_\alpha, u_0, \omega_n\right)$. Hence, the equations for estimating SPPO parameters are rather established with the only variable being the way derivatives are calculated. However, Schoser et al. (2022) expanded the derivatives with terms considering two equally powerful wings. Zero downwash effect from the leading to the trailing wing was assumed while calculating the linearised SPPO approximations as there was no downwash modelled in the eVTOL flight simulator.

3. Results and discussion

3.1. Control inceptors

Figure 3 shows the signals generated by the control inceptors (yoke, throttle and frame levers, right side of all graphs) and their outputs (left side of all graphs) transferred into the numerical flight dynamics model. As mentioned above, the current model assumed a bare airframe, i.e. no control systems implemented, hence the output signals directly followed the input signals with no delay and/or dynamics.

Both yoke-elevon and frame lever-angle control couples have inverted vertical axes on the right side. For the yoke-elevon control couple it is explained by the fact that pushing the yoke forward creates a negative (pitch down) motion, hence a negative pitching moment. It is generally agreed that an aircraft responds positively to a positive control action by a pilot, but negatively to a positive control surface deflection (Cook, 2013), hence the opposite behaviour on the left and right axes. Case with the frame angle is different as the behaviour of the frame lever-angle control couple comes from the pilot sense, i.e. pushing the lever forward it is common sense to expect the rotational
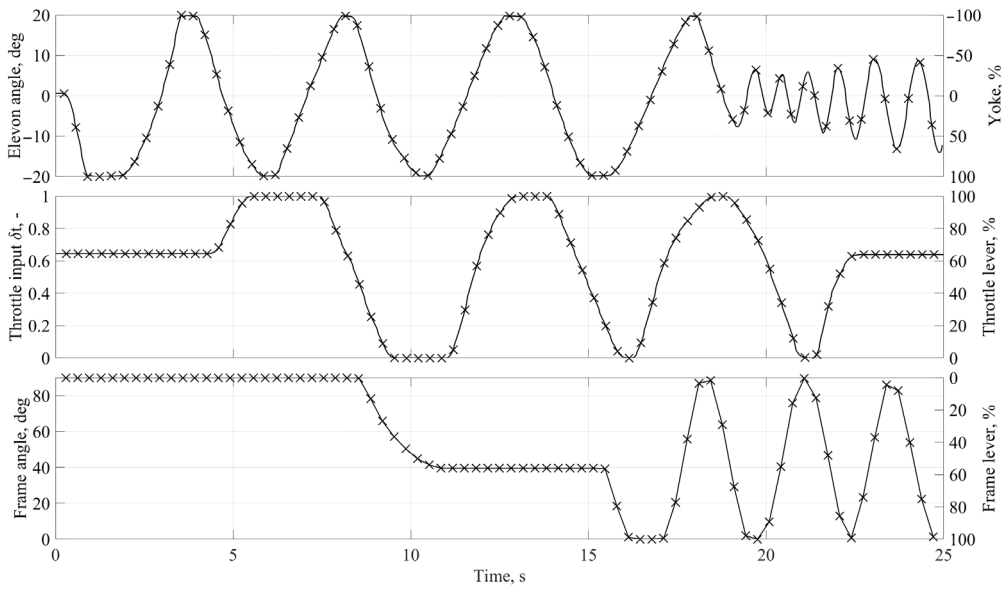
Figure 3. Control inceptor (yoke and levers) signal (×) and control output in simulator (—)

part (frame or, in this case, motors) to rotate from the vertical to the horizontal position. However, the signal of the fuel mixture lever reaches its maximum value when the lever is fully forward and the minimum value when the lever is fully back. Hence, this frame lever-angle control couple must be inverted so that the maximum frame angle, i.e. 90° or vertical position, is reached with the lever being fully back and the minimum frame angle, i.e. 0° or horizontal position, with the lever being fully forward.

Note that all three control couples were scaled by 0.2 (yoke-elevon), 0.01 (throttle lever-input) and 0.9 (frame lever-angle) to transfer the pilot inputs from the cockpit into the flight dynamics model.

3.2. Take-off and transition

Figure 4 shows the transition profile for two different engine (RPM) settings. 90° frame angle represents fully vertical, i.e. thrust-borne, flight mode, while 0° frame angle

represents fully horizontal, i.e. wing-borne, flight mode. The transition between thrust- and wing-borne modes happens in-between.

150 m and 300 m altitudes were achieved in both cases at different times, i.e. flight with higher engine RPM setting reached both altitudes earlier. However, the flight with higher engine RPM overshot the target altitude more significantly, i.e. by 69.5 m versus 19.6 m for the lower engine RPM, while 150 m altitude was reached in 6.2 s for higher RPM versus 10.0 s for lower RPM setting. Hence, the eVTOL with higher RPM setting reached the altitude of 150 m 38.0% quicker, while overshooting the altitude of 300 m 254.6% more than the eVTOL with lower RPM setting.

Paragraph 3.1 of MIL-F-83300 (Chalk et al., 1971) suggests that the concept of "flight envelopes" is not applicable for the transition mode, hence imposing rather qualitative assessment of the handling qualities of VTOL aircraft. The flight test of eVTOL configuration showed that
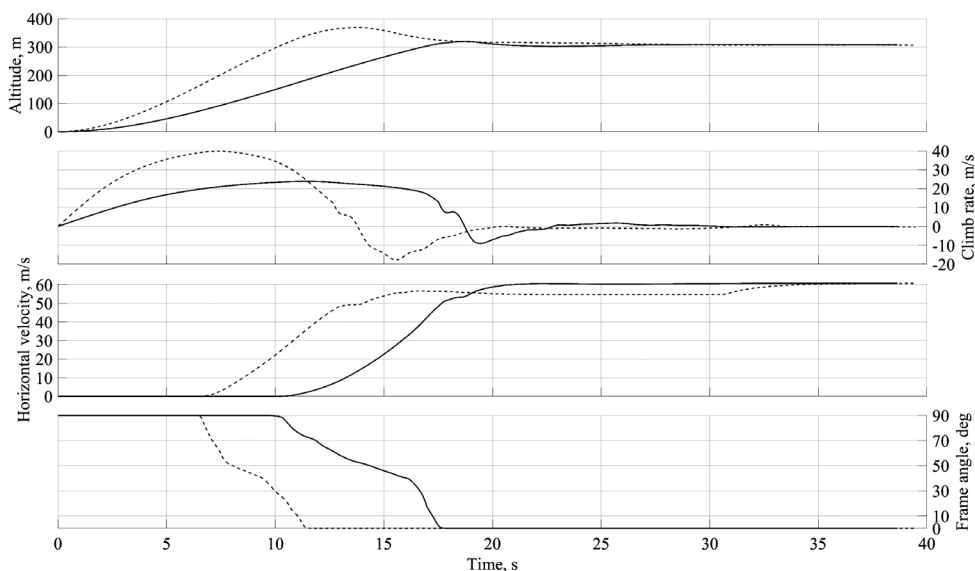

Figure 4. Transition profile (altitude and frame angle) for two engine settings: 1950 RPM (—), 2250 RPM (- -)

adequate controls were available to a pilot for the transition from the vertical (take-off) flight mode to the horizontal (cruise) flight mode and were "easily operated" by a single pilot, which is the requirement 3.4.1 from MIL-F-83300. The tested eVTOL aircraft was "controllable and manoeuvrable" also showed "suitable stability and control feel" during the take-off and transition, hence meeting further requirements VTOL.2135 and VTOL.2145(a) (EASA, 2024).

3.3. Longitudinal short period dynamics

Figure 5 shows the raw test data for the SPPO response of the eVTOL aircraft for two airspeed cases at the same CG position. It is evident that 1) the reference angle of attack α_{ref} was lower, and 2) the reference elevon deflection angle $\delta_{elev_{ref}}$ was lower for the high speed condition. This reflects an expected outcome as the lift force ($L = S \frac{\rho V^2}{2} C_L(\alpha)$, where $C_L = f(\alpha)$) must be maintained for the level flight. The aerodynamic derivative $\frac{dC_L}{d\alpha} = C_{L_\alpha}$ of an airfoil and, hence, of a wing is usually positive, hence α must be reduced to maintain the same lift at a higher velocity. Elevon deflection δ_{elev}, needed to maintain the total pitching moment of zero for a straight and level flight, was also smaller for the higher velocity flight due to the lower AoA needed. However, it is important to notice the need of a trim tab on elevons at this CG configuration as the negative deflection limit has been achieved while inducing SPPO mode. It is also possible to change the working range of elevons, which is now set as $\delta_{elev} \in [-20°; 20°]$, or the CG position to reduce $\delta_{elev_{ref}}$. However, the latter two options were out of scope for this paper.

Figure 5 also shows that the SPPO mode was damped and stable. This supports the flying qualities related requirement VTOL.2145(b), stating that "… no aircraft may exhibit any divergent stability characteristic…" (EASA, 2024). SPPO parameters calculated from the test data are presented in Table 1.

Table 1. Properties of the SPPO mode at different velocities

V_{ref}, m/s	T, s	ω_n, rad/s	ζ, –
53.7 (low)	1.240	5.066	0.217
62.3 (high)	1.096	5.734	0.215

It shows a significantly higher (+13.2%) natural frequency of the SPPO mode for higher velocity flight condition, but very minimal change (–0.9%) in damping ratio. Hence, flying faster did not impact SPPO damping ratio, but increased its natural frequency – the behaviour that is corroborated by the literature for the traditional fixed wing aircraft configurations (Etkin, 2005; Sinha & Ananthkrishnan, 2021). MIL-F-8785C classifies the tested eVTOL aircraft as Class I (light aeroplane) and categorises the flight phase as Cat B (cruise). Based on this information, the tested eVTOL aircraft exhibited Level 1 handling qualities based on the SPPO natural frequency requirements. However, only Level 2 HQs were achieved based on the SPPO damping requirements. This means that only Level 2 ("… adequate to accomplish the mission flight phase…") HQs were achieved by the eVTOL aircraft based on the SPPO mode as it is the usual practice to assign the level of HQs based on the lowest score.

Table 2. Comparison of the non-linear SPPO mode parameters against linearised SPPO approximations

Parameter	V_{ref}, m/s	Flight simulator	Nelson (1998)	Schoser et al. (2022)
ω_n, rad/s	53.7	5.066	4.761	4.769
	62.3	5.734	5.523	5.533
ζ, –	53.7	0.217	0.209	0.258
	62.3	0.215	0.209	0.258

Table 2 compares SPPO parameters calculated from the non-linear flight simulations and linearised SPPO approximations.
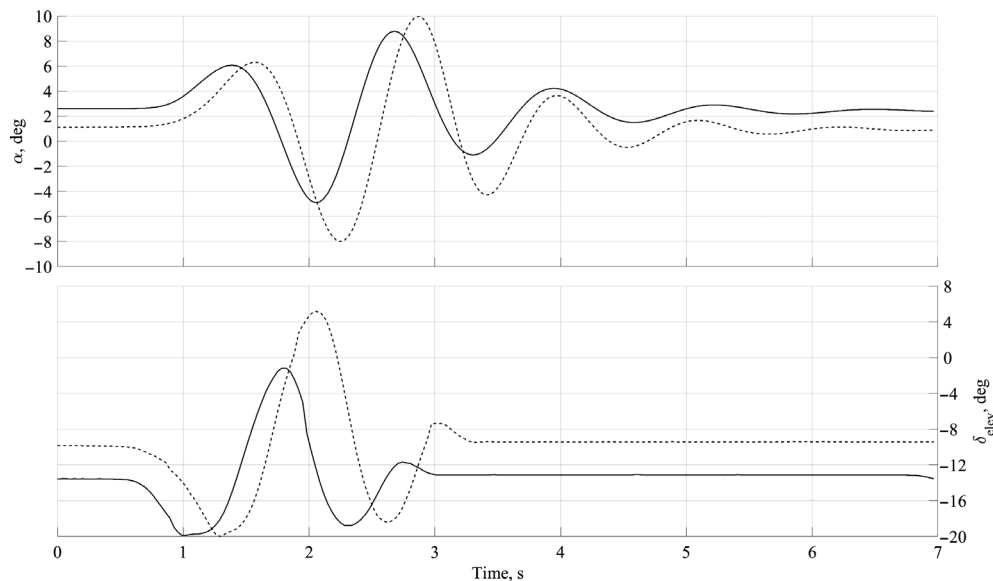

Figure 5. SPPO mode induction and response for low (—) and high (- -) airspeeds

Firstly, both linear approximations predicted similar natural frequency that differed by less than 0.2%. This is understandable as both methods were derived from the same principles and with very similar assumptions. Schoser et al. (2022) updated the traditional tube-and-wing aimed method with assumption more relevant to tandem wing configuration, i.e. derivative M_q assumes equal impact from both forward and rear wings, which is different from the traditional method presented by Nelson (1998) that assumes only the horizontal tailplane affecting the pitching moment as the CG is close to AC of the main wing, leading to a very short moment arm and, hence, small pitching moment produced by the main wing. Also, derivative M_α for the updated method considers impact of the drag force, while the traditional method considers only the lift force generated due to change in AoA.

Comparing the SPPO mode parameters calculated from the flight simulator data against Nelson (1998), flight simulator data estimated 3.8% (high speed case) to 6.4% (low speed case) higher natural frequency. This could be explained by the assumptions made when linearising the equations, e.g. derivative Z_α considers only the impact of the main (forward) wing, while in reality both wings are equally important in the tandem-wing case.

Secondly, it is important to notice that the damping ratio significantly differed between both linearised methods, which is contrary to the natural frequencies. Schoser et al. (2022) predicted 23.5% higher damping ratio value than Nelson (1998). This difference could be mostly related to the calculation of M_q and Z_α derivatives, which account for two large wings rather than considering only horizontal tailplane as the main contributor. Flight simulator data estimated 2.9% (high speed case) to 3.8% (low speed case) higher damping ratio values when compared to Nelson (1998).

4. Conclusions

An increasing number of eVTOL designs requires a flight dynamics testing framework that allows a rapid assessment of their flying and handling qualities at a relatively low cost. Hence, an eVTOL flight simulator, capable of pilot-in-the-loop simulations, has been developed and presented in this paper.

Alsim AL250 FNPT II flight simulator provided the cockpit environment and visuals, while MATLAB/Simulink provided the flight dynamics model. The black throttle lever was chosen to control the rotational speed of the motors and the red mixture lever was chosen to control the propeller incidence angle. Flight dynamics model considered only the linear range of the aerodynamic coefficients and did not model the downwash. Neoptera's eOpter eVTOL aircraft was chosen as a test object for the verification of the simulator.

Verification of the flight simulator was performed in three steps. Firstly, it was shown that signals of the control inputs to the flight dynamics model follow the inputs made by a pilot in the cockpit. Secondly, it was shown that, as expected, the eVTOL with 2250 RPM setting reached the altitude of 150 m 38.0% quicker, while overshooting the altitude of 300 m 254.6% more than the eVTOL with 1950 RPM setting. The qualitative assessment of the eVTOL transition performance against the MIL-F-83300 and SC-VTOL-02 requirements showed adequate controllability and stability of the tested eVTOL aircraft during the transition phase. Finally, the quantitative longitudinal dynamics test of the SPPO mode showed Level 2 handling qualities against the MIL-F-8785C requirements, qualitative definition of which agreed with the pilot's opinion, for the tested eVTOL aircraft. It also showed an increase in SPPO natural fequency with increasing reference velocity, but almost no change in SPPO damping ratio with the same reference velocity change, which is an expected behaviour based on the literature. Comparison of SPPO parameters estimated from simulation data against established linear SPPO approximation by Nelson (1998) showed that both the natural frequency and damping were estimated higher by 3.8–6.4% and 2.9–3.8% accordingly, both differences decreasing with an increasing reference flight velocity. Comparison of linearised SPPO approximations between Nelson (1998) for traditional tube-and-wing aircraft and Schoser et al. (2022) for tandem-wing aircraft showed close estimates for SPPO natural frequency (difference of 0.2%) and significantly different estimates for SPPO damping ratio (difference of 23.5%). Analysis suggested that the main difference between both methods lies in the way the aerodynamic derivatives are calculated. Hence, an extensive analysis into calculating the derivatives for tandem-wing aircraft is suggested.

Funding

Disclosure statement

Author of the paper declares no competing financial, professional, or personal interests from other parties.

References

Abà, A., Barra, F., Capone, P., & Guglieri, G. (2020). Mathematical modelling of gimballed tilt-rotors for real-time flight simulation. *Aerospace*, *7*(9), Article 124. https://doi.org/10.3390/aerospace7090124

Chalk, C. R., Key, D. L., Kroll, J. Jr., Wasserman, R., & Radford, R. C. (1971). *Background information and user guide for MIL-F-83300, military specification – Flying qualities of piloted V/STOL aircraft* (No. AFFDL-TR-70-88). Air Force Flight Dynamics Laboratory.

Churchill, G. B., & Dugan, D. C. (1982). *Simulation of the XV-15 tilt rotor research aircraft* (No. NASA-TM-84222). NASA Ames Research Center.

Cook, M. V. (2013). *Flight dynamics principles: A linear systems approach to aircraft stability and control* (3rd ed.). Butterworth-Heinemann.

Decker, W. A. (2001). Handling qualities evaluation of XV-15 noise abatement landing approaches using a flight simulator. In *The 57th American Helicopter Society Annual Forum*. American Helicopter Society.

Díaz García, G., Seiferth, D., Meidinger, V., Dollinger, D., Nagarajan, P., & Holzapfel, F. (2021). Conduction of mission task elements within simulator flight tests for handling quality evaluation of an eVTOL aircraft. In *AIAA Scitech 2021 Forum* (virtual event). American Institute of Aeronautics and Astronautics. https://doi.org/10.2514/6.2021-1897

Didey, A. (2020). *Tandem wing tail-sitting aircraft with tilting body* (US 2020/0317332 A1). Patentscope.

European Aviation Safety Agency. (2024). *Special Condition for small-category VTOL-capable aircraft* (No. SC-VTOL-02). EASA.

European Aviation Safety Agency. (2012). *Certification Specifications for Aeroplane Flight Simulation Training Devices* (Certification Specifications No. CS-FSTD(A)). EASA.

Etkin, B. (2005). *Dynamics of atmospheric flight*. Dover Publications.

Hartman, E. P., & Biermann, D. (1938). *The aerodynamic characteristics of full-scale propellers having 2, 3, and 4 blades of clark Y and R.A.F. 6 airfoil sections* (No. NACA-TR-640). NACA Langley Aeronautical Laboratory.

Hepperle, M. (2017). *JavaFoil user's guide* (user guide).

Midlands Aerospace Alliance, Lichfields, Achieving the Difference. (2024). *Future flight challenge community integration local planning guidance paper*. Innovate UK.

Moorhouse, D. J., & Woodcock, R. J. (1981). *Background information and user guide for MIL-F-8785C, military specification – Flying qualities of piloted airplanes* (No. AFWAL-TR-81-3109). USAF Wright Aeronautical Laboratories.

Nelson, R. C. (1998). *Flight stability and automatic control* (2nd ed.). WCB/McGraw-Hill.

Padfield, G. D., & White, M. D. (2003). Flight simulation in academia HELIFLIGHT in its first year of operation at the University of Liverpool. *The Aeronautical Journal*, *107*(1075), 529–538. https://doi.org/10.1017/S0001924000013415

Portapas, V., & Cooke, A. K. (2020). Simulated pilot-in-the-loop testing of handling qualities of the flexible wing aircraft. *Aviation 24*(1), 1–9. https://doi.org/10.3846/aviation.2020.12175

Portapas, V., Cooke, A. K., & Lone, M. M. (2016). Modelling framework for flight dynamics of flexible aircraft. *Aviation*, *20*(4), 173–182. https://doi.org/10.3846/16487788.2016.1264719

Portapas, V., & Zaidi, Y. (2022). Framework for developing digital twin prototypes. In *The 2022 NATO Modelling & Simulation Group Symposium: Emerging and Disruptive Modelling and Simulation Technologies to Transform Future Defence Capabilities*. NATO STO.

Portapas, V., Zaidi, Y., Bakunowicz, J., Paddeu, D., Valera-Medina, A., & Didey, A. (2021). Targeting global environmental challenges by the means of novel multimodal transport: Concept of operations. In *The 2021 Fifth World Conference on Smart Trends in Systems Security and Sustainability* (*WorldS4*) (pp. 101–106). IEEE. https://doi.org/10.1109/WorldS451998.2021.9514048

Schoser, J., Cuadrat-Grzybowski, M., & Castro, S. G. (2022). Preliminary control and stability analysis of a long-range eVTOL aircraft. In *The AIAA SCITECH 2022 Forum*. American Institute of Aeronautics and Astronautics. https://doi.org/10.2514/6.2022-1029

Simmons, B. M. (2023). System identification approach for eVTOL aircraft demonstrated using simulated flight data. *Journal of Aircraft*, *60*(4), 1078–1093. https://doi.org/10.2514/1.C036896

Sinha, N. K., & Ananthkrishnan, N. (2021). *Elementary flight dynamics with an introduction to bifurcation and continuation methods* (2nd ed.). CRC Press. https://doi.org/10.1201/9781003096801

Vertical Flight Society. (2024). *eVTOL aircraft directory*. https://evtol.news/aircraft

Zhao, W., Wang, Y., Li, L., Huang, F., Zhan, H., Fu, Y., & Song, Y. (2024). Design and flight simulation verification of the dragonfly eVTOL Aircraft. *Drones*, *8*(7), Article 311. https://doi.org/10.3390/drones8070311

Notations

Abbreviations

AAL – above aerodrome level;
AoA – angle of attack;
CG – centre of gravity;
DoF – degrees of freedom;
eVTOL – electric VTOL;
MTOM – maximum take-off mass;
RPM – revolutions per minute;
SPPO – short period pitching oscillation;
VTOL – vertical take-off and landing aircraft.

Variables

Re – Reynolds number;
T – period;
V – flight velocity;
α – angle of attack;
δ – control input;
ω – frequency;
ζ – damping.

Subscripts

$elev$ – elevon;
n – natural;
ref – reference / trim value.